# NATIONAL ADVISORY COMMITTEE
# FOR AERONAUTICS

## TECHNICAL NOTE 3044

EFFECT OF A RAPID BLADE-PITCH INCREASE ON THE

THRUST AND INDUCED-VELOCITY RESPONSE

OF A FULL-SCALE HELICOPTER ROTOR

By Paul J. Carpenter and Bernard Fridovich

Langley Aeronautical Laboratory
Langley Field, Va.

### NACA

Washington

November 1953

NATIONAL ADVISORY COMMITTEE FOR AERONAUTICS

TECHNICAL NOTE 3044

EFFECT OF A RAPID BLADE-PITCH INCREASE ON THE

THRUST AND INDUCED-VELOCITY RESPONSE

OF A FULL-SCALE HELICOPTER ROTOR

By Paul J. Carpenter and Bernard Fridovich

SUMMARY

A method has been proposed for predicting the effect of a rapid blade-pitch increase on the thrust and induced-velocity response of a helicopter rotor. General equations have been derived for the ensuing motion of the helicopter. These equations yield time histories of thrust, induced velocity, and helicopter vertical velocity for given rates of blade-pitch-angle changes and given rotor-angular-velocity time histories.

The results of the method have been compared with experimental results obtained with a rotor mounted on the Langley helicopter test tower. The calculated and experimental results are in good agreement, although, in general, the calculated thrust-coefficient overshoots are about 10 percent greater than those obtained experimentally.

INTRODUCTION

One of the methods currently used to get an overloaded helicopter airborne is the maneuver commonly referred to as the "jump take-off" or "engine overspeed take-off." This maneuver is a take-off with a flight path initially vertical, effected by the release of excess kinetic energy stored in the rotor. The rotor is initially accelerated at or near a blade pitch angle of $0^\circ$ to a rotor speed greater than its normal speed. At this overspeed condition, the blade pitch is suddenly increased to its normal value or higher and the consequent rotor thrust, being greater than the weight of the machine, lifts it vertically from the ground. During the take-off, the rotor decelerates, the thrust returns to its normal value, and the pilot must gain sufficient forward speed to stay airborne with the power available.

The purpose of this paper is to study the aerodynamic factors affecting the transient rotor thrust and induced-flow buildup during a

jump take-off.  A method is proposed for predicting the general motion
of a helicopter following a rapid collective-pitch increase such as may
be encountered in a jump take-off for given rates of blade-pitch change
and for given rotor-angular-velocity time histories.  The equations
yield time histories of thrust, induced velocity, helicopter velocity,
and helicopter displacement.

A comparison of the results of this method with the experimental
results obtained for a rotor mounted on the Langley helicopter test
tower is presented.

SYMBOLS

R        blade radius, ft

b        number of blades

c        blade section chord, ft

r        radial distance to blade element, ft

$c_e$        equivalent blade chord, $\dfrac{\displaystyle\int_0^R cr^2\,dr}{\displaystyle\int_0^R r^2\,dr}$, ft

$c_1 = \dfrac{\displaystyle\int_0^R cr\,dr}{\displaystyle\int_0^R r\,dr}$, ft

$c_2 = \dfrac{\displaystyle\int_0^R cr^3\,dr}{\displaystyle\int_0^R r^3\,dr}$, ft

a        slope of curve of section lift coefficient against section angle
         of attack (radian measure), assumed to be 5.73

$I_1$        blade moment of inertia about flapping hinge, slug-ft$^2$

$M_T$     blade thrust moment about horizontal hinge, lb-ft

$M_W$     blade weight moment about horizontal hinge, lb-ft

m         apparent additional mass of air influenced by rotor disk,

$\qquad$ $0.637\rho \, \frac{4}{3}\pi R^3$, slugs

$m_b$     total mass of rotor blades, slugs

$m_H$     helicopter mass (does not include blade mass), slugs

g         acceleration due to gravity, ft/sec$^2$

t         time, sec

$l$         distance of blade center of mass from flapping hinge, ft

$\rho$         mass density of air, slugs/cu ft

v         induced inflow velocity at rotor, ft/sec

T         rotor thrust, lb

$T_m$     measured rotor thrust, lb

$\Omega$         rotor angular velocity, radians/sec

$\theta$         blade-section pitch angle measured from line of zero lift, radians

$\beta$         blade flapping angle; angle between blade span axis and plane
          perpendicular to axis of no feathering, radians

$V_v$       vertical velocity of helicopter, ft/sec

$\eta$         thrust correlation factor between simple blade-element—momentum
          theory and strip analysis

$\tau$         thrust-moment correlation factor between simple blade-element—
          momentum theory and strip analysis

Subscripts:

s         steady-state conditions

r         conditions existing at a blade element  r  distance from center
          line of rotation

a        adjusted value to correlate simple blade-element—momentum theory
            to strip analysis

    Dots over a symbol indicate derivatives with respect to time.


## APPARATUS AND TESTS


    The helicopter rotor used was a conventional three-blade rotor with
flapping hinges located at the center of rotation and drag hinges offset
about 9 inches from the center of rotation.  The blade radius was 19 feet.
The blades were plywood covered and untwisted and had NACA 23015 airfoil
sections and the rotor solidity was 0.042.  A plan-form view of one of
the test rotor blades is shown in figure 1.

    Experimental data recorded for these tests were rotor angular
velocity, rotor thrust, blade pitch angle, blade flapping angle, and the
induced velocities in the wake beneath the rotor.  A description of the
test methods, except for the technique used in measuring the induced
velocities, is given in reference 1.  The induced velocities were meas-
ured with small calibrated windmill anemometers for the steady-state con-
ditions.  For transient conditions, the wake velocities were obtained by
measuring the drag of balsa-wood paddles (approximately 4 inches square)
mounted on a horizontal bar about 2 feet below the rotor blades.  The
paddles were mounted on strain-gage beams and their response to a change
in induced velocity was recorded by an oscillograph.  The balsa-wood
paddles gave almost instantaneous indications of flow changes, whereas
the windmill anemometers had considerable lag in measuring transient air
velocities.

    As an aid in visualizing the flow changes and in order to supplement
the force and blade-motion data recorded by the oscillograph, smoke
grenades were placed at 4-foot intervals on a boom about 4 feet above the
rotor.  All the release pins on the smoke grenades could be pulled simul-
taneously at the start of a test run.  A high-speed 16-millimeter motion-
picture camera was used to photograph the smoke streamers during both
steady-state and transient wake conditions.

    The slower rates of blade-pitch increase were accomplished by using
electric-motor-driven actuators, whereas the very rapid rates were accom-
plished by using a spring and trigger mechanism on the pitch control.  The
rates of pitch increase that were obtained varied from 6° to 200° per
second.

    The data presented are for the representative cases of blade-pitch
change of 0° to 12°, except for a few tests in which the blade-pitch

change was $0^O$ to $3^O$, $0^O$ to $6^O$, and $0^O$ to $9^O$ to determine the effect on the thrust overshoot of changing the magnitude of the blade-pitch change.

## ANALYSIS

The complete description of the general motion of a helicopter following a collective blade-pitch-angle increase must include time histories of $v$, $V_v$, and $\beta$. In order to isolate the aerodynamic forces on the rotor, time histories of blade pitch angle $\theta$ and rotor speed $\Omega$ are assumed to be given. Three equations, the simultaneous solution of which yields information describing the general motion of the helicopter, are derived.

### Thrust Equations

Momentum theory. - For a helicopter moving vertically with constant velocity $V_{v_s}$, the rotor thrust as given by simple momentum theory is

$2\pi R^2 \rho v_s \left(v_s + V_{v_s}\right)$, where $v_s$, the steady-state induced velocity, is

assumed uniform over the rotor disk. This expression for thrust is valid only for steady-state conditions and is not immediately applicable to the transient phenomena which are the primary concern of this paper. An expression for the thrust of a helicopter rotor during the transient airflow conditions following a sudden increase in blade pitch angle is now developed.

Consider a stationary rotor the blades of which, initially whirling at zero pitch angle, are suddenly given a positive pitch angle $\theta$. Before the pitch change, no air was passing through the rotor disk. As soon as the pitch reaches a positive value, the induced velocity $v$ starts to build up. If the induced velocity is assumed to be uniform over the rotor disk, the initial flow field is exactly analogous to the flow field produced by an impervious disk which is moved normal to its plane. The "apparent additional mass" of fluid associated with an accelerating impervious disk is given in reference 2 as 63.7 percent of the mass of fluid in the circumscribed sphere. Although the analogy with the accelerating impervious disk is not strictly valid after a slipstream has formed, it will nevertheless be assumed that this same apparent additional mass is associated with the rotor disk and must be accelerated during the induced-velocity buildup. The force required to accelerate this mass of air is $m\dot{v}$, where $m$ is the apparent additional mass associated with the rotor. It is proposed that during the unsteady conditions the aerodynamic loading on the rotor disk be written as

$$T = m\dot{v} + 2\pi R^2 \rho v \left(v + V_v\right) \tag{1}$$

where $v$ is the instantaneous induced velocity.

The equation is as yet incomplete, and further modifications are made in the course of the analysis. This same procedure, that of revising familiar equations, is used throughout the analysis.

An additional term is added to equation (1) to allow for blade flapping. In equation (1), $V_v$ is the vertical velocity of the rotor hub, which for a rotor whose blades are not flapping is the same as the velocity of the rotor disk. For a rotor with flapping blades, however, this is not the case. The velocity of the rotor disk relative to free air can be expressed as the velocity of the hub plus the velocity of the rotor disk relative to the hub. The latter terms can be found by considering annular elements of the rotor disk, each moving with a different velocity $\dot{\beta}r$ where $\dot{\beta}$ is the angular velocity of the flapping blades. An integration over the rotor disk divided by the rotor-disk area yields the average velocity of the rotor disk relative to the hub, $\frac{2}{3}\dot{\beta}R$. The complete expression for the instantaneous thrust is finally

$$T = m\dot{v} + 2\pi R2\rho v \left(v + V_v + \frac{2}{3}\dot{\beta}R\right) \tag{2}$$

This equation, although admittedly not exact during the whole of the induced-velocity buildup because the flow fields of the impervious disk and helicopter rotor are not strictly analagous, does, however, fit the end points, that is, at the moment an induced velocity appears, and at the final steady state.

The rotor thrust is a dependent variable (depending on $v$, $\dot{\beta}$, and $V_v$), which can be eliminated by equating the thrust expressions as given by momentum and blade-element theories. The expression for the instantaneous thrust as given by a modified blade-element theory is developed next.

Blade-element theory. - The differential rotor thrust can be written in terms of local velocities and angles of attack as

$$dT = \frac{1}{2} b\rho\Omega^2 r^2 ac \left(\theta - \frac{v_r}{\Omega r} - \frac{V_v}{\Omega r} - \frac{\dot{\beta}}{\Omega}\right) dr \tag{3}$$

where the expression for the angle of attack contains terms to include the effects of the induced velocity, the vertical velocity of the helicopter, and the flapping motion of the blades.

Integrating equation (3) with $v$ and $\theta$ considered invariant with respect to $r$ gives

$$T = \frac{1}{2}b\rho\Omega^2 a \left[\left(\theta - \frac{\dot{\beta}}{\Omega}\right)\int_0^R cr^2 dr - \left(\frac{v}{\Omega} + \frac{V_v}{\Omega}\right)\int_0^R cr\, dr\right] \tag{4}$$

or

$$T = \frac{1}{6}b\rho\Omega^2 a c_e R^3 \left(\theta_r - \frac{3}{2}\frac{c_1}{c_e}\frac{v}{\Omega R} - \frac{3}{2}\frac{c_1}{c_e}\frac{V_v}{\Omega R} - \frac{\dot{\beta}}{\Omega}\right) \tag{5}$$

where

$$c_e = \frac{\displaystyle\int_0^R cr^2 dr}{\displaystyle\int_0^R r^2 dr}$$

and

$$c_1 = \frac{\displaystyle\int_0^R cr\, dr}{\displaystyle\int_0^R r\, dr}$$

Equations (2) and (5) could now be equated to yield one of the three equations necessary for the solution of the general problem. Before this step is taken, however, a method is proposed to minimize the errors that naturally result from assuming $v$ uniform over the rotor disk.

Correlation of thrust. - The details of the procedure for finding thrusts and moments considering $v = f(r)$ can be found in reference 3. Only a brief outline is given here.

The equilibrium thrust on a blade element as expressed by the momentum and blade-element theories can be equated to give

$$dT_s = 2\pi\rho r\left(v_{r_s} + V_{v_s}\right)2v_{r_s}dr = \frac{1}{2}\,b\rho\Omega^2 r^2 a\left(\theta - \frac{v_{r_s}}{\Omega r} - \frac{V_{v_s}}{\Omega r}\right)dr \qquad (6)$$

After simplifying and rearranging terms there results a quadratic in $v_r$ whose solution is

$$v_{r_s} = \left(\frac{V_{v_s}}{2} + \frac{bca\Omega}{16\pi}\right)\left[-1 + \sqrt{1 + \frac{2\Omega r\left(\theta - \frac{V_{v_s}}{\Omega r}\right)}{\frac{4\pi V_{v_s}^2}{bca\Omega} + V_{v_s} + \frac{bca\Omega}{16\pi}}}\right] \qquad (7)$$

If values of $v_{r_s}$ computed at various radial stations are substituted back into equation (6), values of $\frac{dT}{dr}$ can be obtained. A graphical integration yields the total thrust.

Equations (2) and (5) taken at equilibrium can be combined to give

$$\frac{1}{6}\rho b\Omega^2 ac_eR^3\left(\theta - \frac{3}{2}\frac{c_1}{c_e}\frac{v_s}{\Omega R} - \frac{3}{2}\frac{c_1}{c_e}\frac{V_{v_s}}{\Omega R}\right) = 2\pi R^2\rho v_s\left(v_s + V_{v_s}\right) = T_s \qquad (8)$$

This equation can be solved for $v_s$. If $v_s$ is now substituted back into equation (8), a value of the thrust will be found which is appreciably different from the value found by using $v_{r_s}$ as given by equation (7).

It is now proposed to alter equation (8) so that it will yield an average velocity $v_a$ that will give a value for the thrust consistent with the value found by using $v_{r_s}$ obtained from equation (7).

In order to accomplish this change, a constant factor $\eta$ is introduced into equation (8) as follows:

$$T_s = \frac{1}{6}\rho b\Omega^2 a c_e R^3 \left(\theta - \frac{3}{2}\eta\frac{c_1}{c_e}\frac{v_a}{\Omega R} - \frac{3}{2}\frac{c_1}{c_e}\frac{V_{v_s}}{\Omega R}\right) \tag{9}$$

$$= 2\pi R^2 \rho v_a \left(v_a + V_{v_s}\right) \tag{9a}$$

Let $T_s$ be equal to the thrust obtained by using $v_{r_s}$ and solve for $\dot{v}_a$ by using the expression for thrust as given by equation (9a). If this value of $v_a$ is next substituted into the expression for thrust as given by equation (9), the value of $\eta$ can be found. The insertion of $\eta$ insures compatible values of thrust by using $v_s$ (now called $v_a$) or $v_{r_s}$.

Although $\eta$ was computed for the steady-state condition, it is now proposed that this same factor be employed during unsteady conditions. With this assumption the expressions for the instantaneous thrust from blade-element (eq. (9)) and momentum theories (eq. (2)) can be equated and rewritten as

$$\frac{1}{6}\rho b\Omega^2 a c_e R^3 \left(\theta - \frac{3}{2}\eta\frac{c_1}{c_e}\frac{v}{\Omega R} - \frac{3}{2}\frac{c_1}{c_e}\frac{V_v}{\Omega R} - \frac{\dot{\beta}}{\Omega}\right) = m\dot{v} + 2\pi R^2\rho v\left(v + V_v + \frac{2}{3}\dot{\beta}R\right) \tag{10}$$

Equation (10) is the first equation of the system of equations necessary for the solution of the general problem. The blade-flapping equations are now derived.

### Blade-Flapping Equations

Each blade is acted on by air forces, inertia forces, and its weight. The sum of the moments caused by these forces equals the moment of inertia of the blade multiplied by its angular acceleration.

<u>Moments due to air forces</u>. - The moments due to air forces are found by integrating the moments caused by the blade elements. The steps are outlined briefly as follows:

$$dM_T = \frac{1}{2} \rho \Omega^2 a c r^3 \left( \theta - \frac{v}{\Omega r} - \frac{V_v}{\Omega r} - \frac{\dot{\beta}}{\Omega} \right) dr \tag{11}$$

Upon integrating, $v$ being kept uniform over the rotor disk, there results the total moment, now considered as an instantaneous value,

$$M_T = \frac{1}{8} \rho \Omega^2 a c_e R^4 \left( \frac{c_2}{c_e} \theta - \frac{4}{3} \frac{v}{\Omega R} - \frac{4}{3} \frac{V_v}{\Omega R} - \frac{c_2}{c_e} \frac{\dot{\beta}}{\Omega} \right) \tag{12}$$

where

$$c_2 = \frac{\displaystyle\int_0^R c r^3 dr}{\displaystyle\int_0^R r^3 dr}$$

For steady-state conditions, the thrust moment calculated by using equation (12) (where $v$ is uniform over the rotor disk) is different from the moment calculated by using $v_{r_s}$. This difference is eliminated by introducing a constant factor $\tau$ into equation (12) at equilibrium as follows:

$$M_{T_s} = \frac{1}{8} \rho \Omega^2 a c_e R^4 \left( \frac{c_2}{c_e} \theta - \frac{4}{3} \tau \frac{v_a}{\Omega R} - \frac{4}{3} \frac{V_{v_s}}{\Omega R} \right) \tag{13}$$

In order to obtain $\tau$ let $M_{T_s}$ equal the value found by integrating $\frac{dT}{dr} r$ from equations (6) and (7) and let the value of $v_a$ be considered as the value obtained from equation (9a). The value of $\tau$ can be immediately obtained from equation (13). The instantaneous thrust moment can be written as

$$M_T = \frac{1}{8} \rho \Omega^2 a c_e R^4 \left( \frac{c_2}{c_e} \theta - \frac{4}{3} \tau \frac{v}{\Omega R} - \frac{4}{3} \frac{V_v}{\Omega R} - \frac{c_2}{c_e} \frac{\dot{\beta}}{\Omega} \right) \tag{14}$$

Moments due to inertia forces and weight. - The moments due to inertia forces are the familiar centrifugal force moments $(I_1 \Omega^2 \beta)$ and one

other caused by the vertical acceleration of the helicopter. The magnitude of this moment can be readily found. Each blade-mass element dm is acted on by an inertia force **directed** oppositely to the helicopter acceleration and equal to $\dot{V}_v$ dm where $\dot{V}_v$ is the vertical acceleration of the helicopter. (See fig. 2.) The moment can therefore be written as $M_W \dot{V}_v \frac{1}{g}$. The weight moment $M_W$ needs no comment.

Flapping-motion equation. - The flapping-motion equation of the blades is

$$I_1 \ddot{\beta} = \frac{1}{8} \rho \Omega^2 ac_e R^4 \left( \frac{c_2}{c_e} \theta - \frac{4}{3} \tau \frac{v}{\Omega R} - \frac{4}{3} \frac{V_v}{\Omega R} - \frac{c_2}{c_e} \frac{\dot{\beta}}{\Omega} \right) -$$

$$I_1 \Omega^2 \beta - M_W \left( 1 + \frac{1}{g} \dot{V}_v \right) \tag{15}$$

The equation describing the motion of the helicopter itself is now developed.

## Helicopter-Motion Equation

The appearance of lift on the blades results in their immediate angular acceleration $\ddot{\beta}$ about the flapping hinge. If $\beta$ is assumed small, this motion produces an acceleration of the rotor center of mass, relative to the hub, of magnitude $l\ddot{\beta}$ in the direction of the rotor axis, where $l$ is the distance of the blade center of mass from the flapping hinge. At the same time, the helicopter itself has an acceleration $\dot{V}_v$. The equation of motion can be written as

$$m_b \left( \dot{V}_v + l\ddot{\beta} \right) + m_H \dot{V}_v = T - \left( m_b + m_H \right) g \tag{16}$$

which upon rearrangement of the terms gives

$$\left(m_b + m_H\right)\dot{V}_v = T - \left(m_b + m_H\right)g - m_b l\ddot{\beta} \qquad (17)$$

where $T$ is the thrust given by either side of equation (10), and $m_H$ is the mass of the helicopter without the blades. A schematic diagram of the forces acting on the helicopter is shown in figure 2.

For a maneuver such as a jump take-off, equation (16) applies only when the helicopter is airborne. Before this time, the ground will exert forces so that $\dot{V}_v$ cannot be negative.

It should be pointed out that, although the equations are general, the employment of the momentum theory restricts the range to where this theory is applicable. The assumption of infinite blade-bending stiffness is a severe simplification and results in overly large inertia forces. It will be noted that many of the equations contain implicitly the assumption of an untwisted blade. This restriction can be eliminated with small error by taking $\theta$ for a twisted blade at the $\frac{3}{4}R$ point.

## Solution of Equations

The system of differential equations (10), (15), and (17) can be solved simultaneously by numerical methods, if values of $\theta$ and $\Omega$ against time are given. Time histories of the variables $v$, $\beta$, $V_v$, and their derivatives result, from which the thrust at any instant can be computed.

For the experiments performed on the Langley helicopter tower, the physical arrangements permit a simplification of the equations. The rotor hub is stationary so that equation (17) is eliminated from the system of equations and the others are suitably modified. The equations to be solved simultaneously are

$$m\dot{v} + 2\pi R^2 \rho v \left(v + \frac{2}{3}\dot{\beta}R\right) = \frac{1}{6}\rho b \Omega^2 a c_e R^3 \left(\theta - \frac{3}{2}\eta \frac{c_1}{c_e} \frac{v}{\Omega R} - \frac{\dot{\beta}}{\Omega}\right) \qquad (18)$$

and

$$I_1\ddot{\beta} + I_1\Omega^2\beta = \frac{1}{8}\rho\Omega^2 ac_e R^4\left(\frac{c_2}{c_e}\theta - \frac{4}{3}\tau \frac{v}{\Omega R} - \frac{c_2}{c_e}\frac{\dot{\beta}}{\Omega}\right) - M_W \tag{19}$$

The thrust felt at the rotor hub is given by a modified form of equation (17) as

$$T_m = m\dot{v} + 2\pi R^2\rho v\left(v + \frac{2}{3}\dot{\beta}R\right) - m_b l\ddot{\beta} \tag{20}$$

The value is found by inserting values of $v$, $\dot{\beta}$, and $\ddot{\beta}$ obtained by a simultaneous solution of equations (18) and (19).

In order to be consistent with other helicopter analyses all integrations for thrust purposes are performed to only 97 percent of the geometrical radius to allow for tip losses.

The system of equations for the specific cases presented in this report were solved by the Bell Telephone Laboratories X-66744 relay computer at the Langley Laboratory. The time interval used for the numerical solution must be small enough to insure that a further reduction will not appreciably affect the results. For the slowest rate of blade-pitch increase presented (fig. 3(d)), it was found that a reduction in time interval from 0.1 second to 0.05 second produced marked changes in the curves of $\dot{\beta}$ and $\ddot{\beta}$ against time but produced only negligible changes in the curves of $\beta$, $V_v$, and $C_T$ against time. It can be inferred from this behavior that for the slow rate of blade-pitch increase $\dot{\beta}$ and $\ddot{\beta}$ exert little influence on the values of $\beta$, $V_v$, and $C_T$. The time intervals used in the curves presented are as follows: figure 3(a), $\Delta t = 0.025$ second; figure 3(b), $\Delta t = 0.020$ second; figure 3(c), $\Delta t = 0.020$ second; figure 3(d), $\Delta t = 0.050$ second. From the preceding remarks it can be seen that the time intervals used for figures 3(b), 3(c), and 3(d) were unnecessarily small to yield reasonably accurate values of $V_v$, $\beta$, and $C_T$.

## RESULTS AND DISCUSSION

A comparison of the time histories of the calculated and experimental rotor response to pitch increases from $0^\circ$ to $12^\circ$ is shown in figure 3 for four rates of increase from $6^\circ$ to $200^\circ$ per second. The curves in figure 3(a) indicate that the overshoot of the experimental rotor thrust coefficient for the rapid blade-pitch increase may be nearly twice the normal thrust coefficient. The magnitude and overshoot of thrust coefficient is slightly less than those calculated. The larger predicted value is probably due to the assumption that the rotor blades had infinite bending stiffness; this assumption results in larger inertia forces than for a practical blade. Comparison of the experimental and calculated flapping-angle displacement indicates good agreement. The experimental blade-pitch changes exceeded, for a short duration, the $12^\circ$ blade-pitch change on which the calculated values are based; however, other records of $200^\circ$ to $400^\circ$ per second rapid blade-pitch changes without pitch overshoot indicated the same overshoot of the thrust coefficient. Rates of blade-pitch change as high as $400^\circ$ per second were obtained that had almost the identical thrust-coefficient variation with time as the somewhat slower rates of $180^\circ$ to $200^\circ$ per second.

It can be seen from these results that the thrust-coefficient overshoot is of very short duration. The thrust-coefficient overshoot decreases about 80 percent in one rotor revolution. The time for the induced velocity to reach its full value is also very small and, for this rotor, less than 1 second for the very rapid rates of pitch increase.

Figures 3(b), 3(c), and 3(d) show comparisons of calculated and experimental time histories for slower rates of blade-pitch increase of $48^\circ$ to $6^\circ$ per second. A comparison of the calculated and experimental curves shows good agreement for both flapping-angle displacements and thrust coefficients. In general, the curves indicate that the time lag between full pitch and full induced velocity is less than 1 second. For a pitch rate of $48^\circ$ per second (fig. 3(b)), which is thought to be the maximum rate at which a pilot can move the controls (based on unpublished CAA and NACA tests), the time lag between full pitch and full induced velocity is approximately 0.7 second, whereas at still a slower rate of $20^\circ$ per second (fig. 3(c)), the time lag is about 0.4 second. For the most rapid rate of blade-pitch increase (fig. 3(a)), the blade inertia accounts for about 38 percent of the total maximum thrust and decreases to about 2 percent of the total maximum thrust for the slowest rate of blade-pitch increase (fig. 3(d)).

The predicted thrust-coefficient overshoot for the slower rates of blade-pitch increase ($6^\circ$ to $48^\circ$ per second) is generally about 10 percent higher than the experimental values. This overestimate is probably due to the simplifying assumptions used in the calculations; however, the method is sufficiently accurate for this study and, at the same time, greatly reduces the labor of calculations.

Photographs taken of the flow patterns formed by the streamers from smoke grenades, spaced at 4-foot intervals, during a very rapid pitch change of approximately 200° per second are presented in figure 4. Since the rotor blade did not photograph clearly, the approximate location of the rotor blade has been drawn in. The horizontal division line at the rotor-hub height that divides the light and dark areas is the horizon. The photographs show a large vortex, such as might be expected from the initial motion of an impervious disk, is quickly generated by the individual blade-tip vortex filaments and is rapidly carried downstream as the wake velocity builds up to its normal value. The photographs indicate that the induced-velocity flow builds up first at the rotor tips and then proceeds inboard. The lag between the first indication of induced flow at the blade tips and at a position of about 0.25R was about 0.3 second or slightly greater than the time for one rotor revolution. This result is contrary to the assumption of uniform buildup along the radius on which the calculations are based. This inboard progression of the induced flow appears to be a secondary effect and does not appreciably affect the results as will be shown in the comparison of calculated and experimental values.

The same general pattern of the large vortex was noted for the slower rates of blade-pitch increase, except that it was not as pronounced as that for the very rapid blade-pitch increases.

Figure 5 shows the comparison of calculated and experimental ratios of maximum rotor thrust coefficient to final rotor thrust coefficient. Good agreement is obtained over the total range of rates of blade-pitch increase and magnitudes of blade-pitch change of 3°, 6°, 9°, and 12°, although, in general, the calculated thrust overshoots are about 10 percent greater than those determined experimentally.

## SUMMARY OF RESULTS

An experimental determination of the response of the thrust and induced velocity of a helicopter rotor to various rates of collective blade-pitch increase has been conducted on the Langley helicopter test tower. Experimental results are compared with calculations based on the concept of an "apparent additional mass" of air influenced by the rotor disk. On the basis of this investigation, the following results were obtained:

1. The time histories of the calculated and experimental thrust coefficients and induced-velocity buildup are in good agreement for

various rates of blade-pitch increase although the predicted values are about 10 percent greater than those experimentally determined.

2.  During a rapid blade-pitch increase, the induced velocity reaches its full value less than 1 second after the pitch reaches its final value.

3.  The thrust-coefficient overshoot following a very rapid pitch increase is about twice the value of the normal thrust; however, the duration is very short.

Langley Aeronautical Laboratory,
     National Advisory Committee for Aeronautics,
          Langley Field, Va., August 4, 1953.

### REFERENCES

1. Carpenter, Paul J.:  Effect of Wind Velocity on Performance of Helicopter Rotors As Investigated With the Langley Helicopter Apparatus.  NACA TN 1698, 1948.

2. Munk, Max M.:  Some Tables of the Factor of Apparent Additional Mass. NACA TN 197, 1924.

3. Gessow, Alfred, and Myers, Garry C., Jr.:  Aerodynamics of the Heli- copter.  The Macmillan Co., c.1952, ch. 4, pp. 67-68.
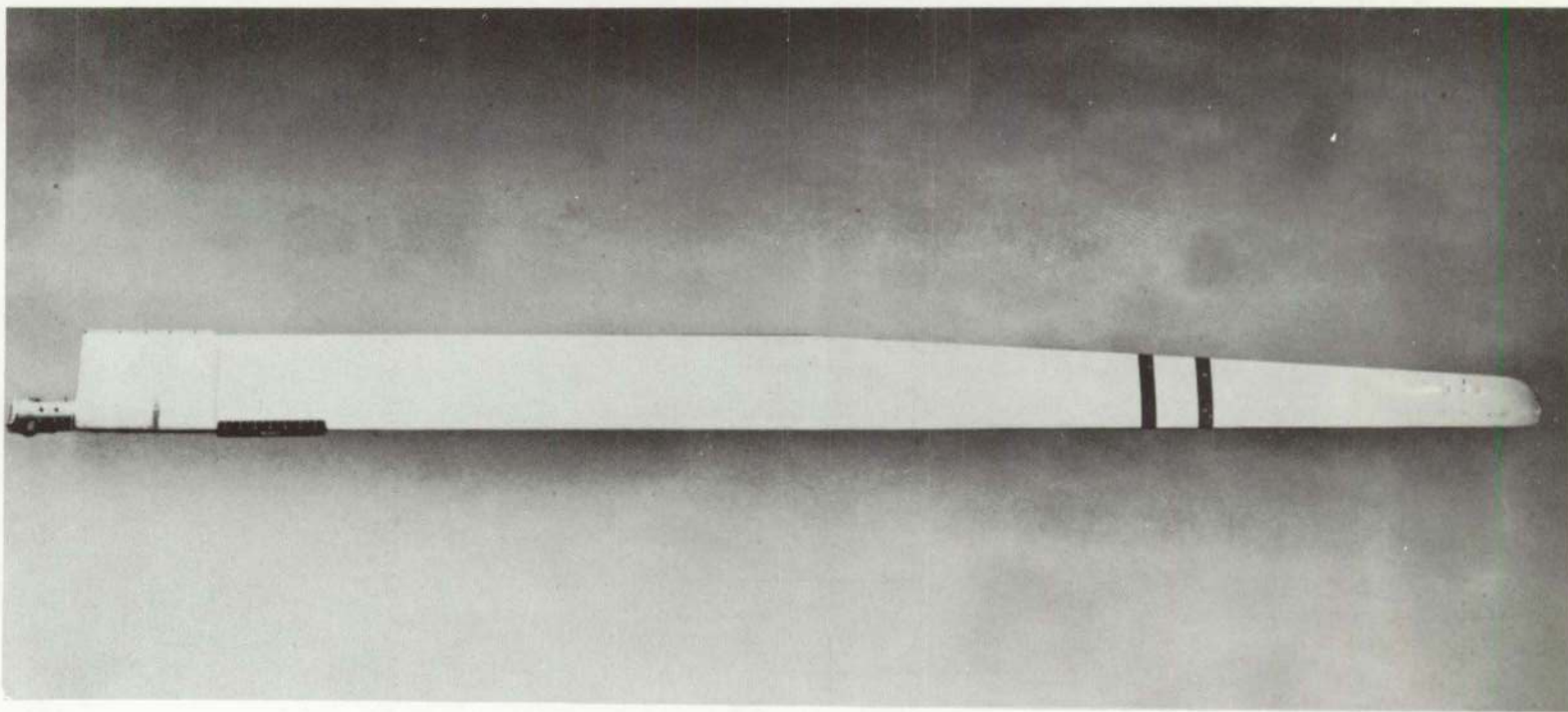
L-40877.1

Figure 1.- Plan-form view of a test rotor blade.

$$\frac{T}{b}$$

$$I_1\Omega^2\beta$$

$$\frac{m_b}{b}(g + \dot{V}_v + l\ddot{\beta})$$

$$T - m_b(g + \dot{V}_v + l\ddot{\beta})$$

$$m_H(g + \dot{V}_v)$$

NACA
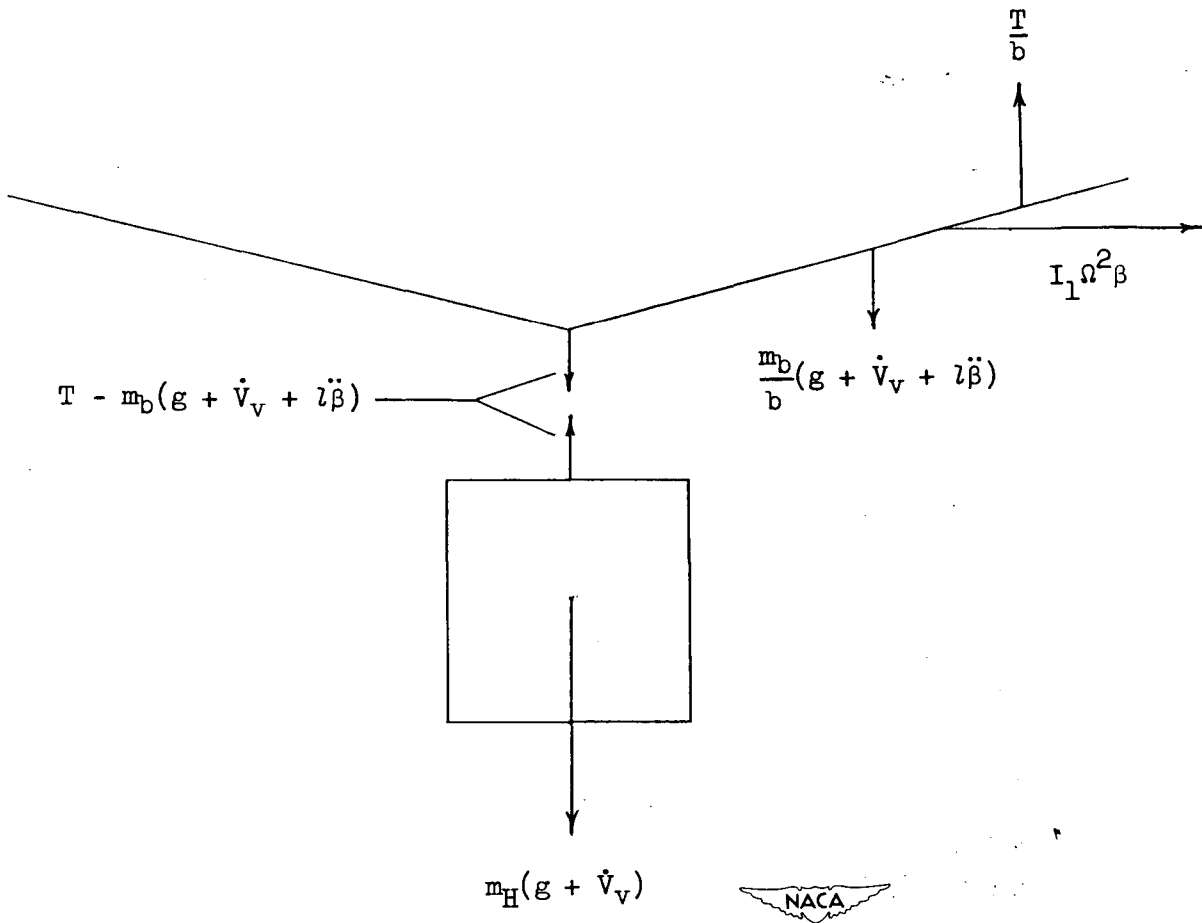
Figure 2.- Schematic diagram showing forces acting on helicopter.
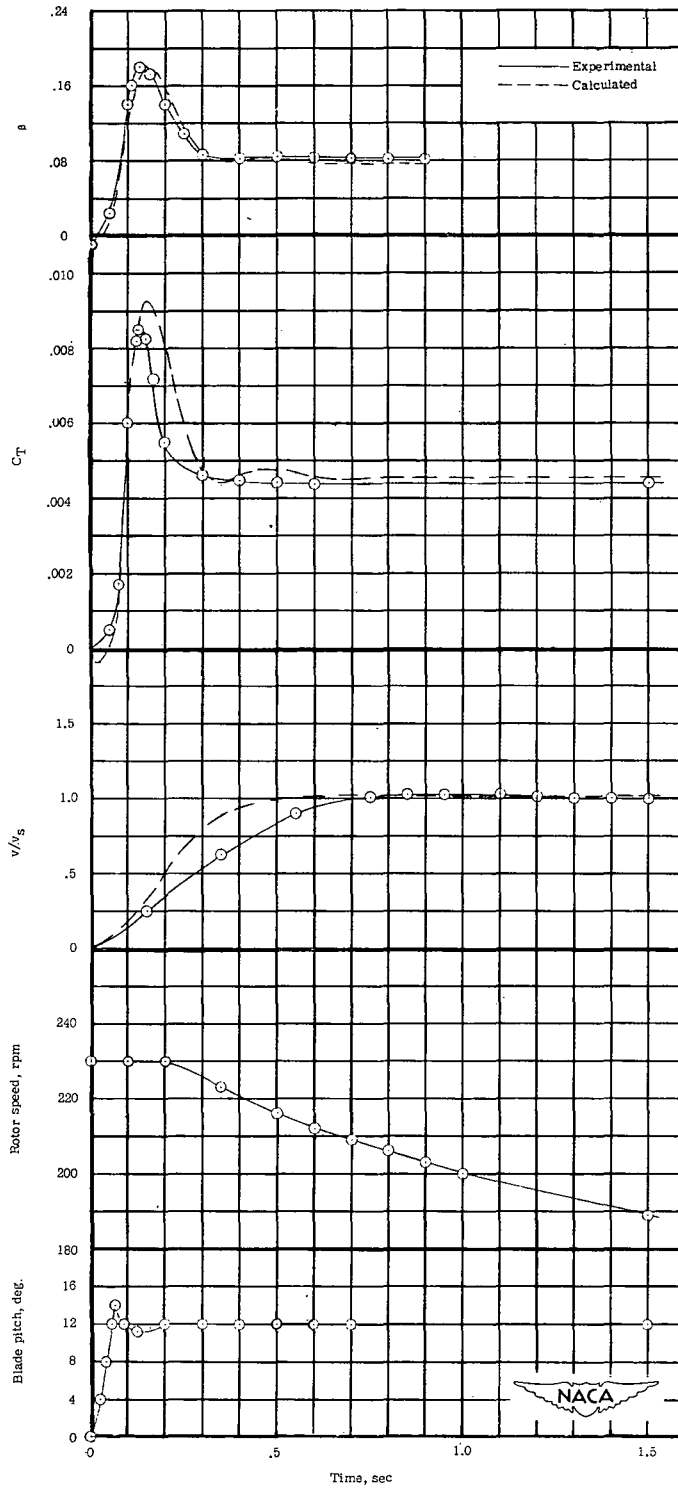
(a) Rate of pitch increase of about 200° per second.

Figure 3.- Time histories of various rates of pitch increase.
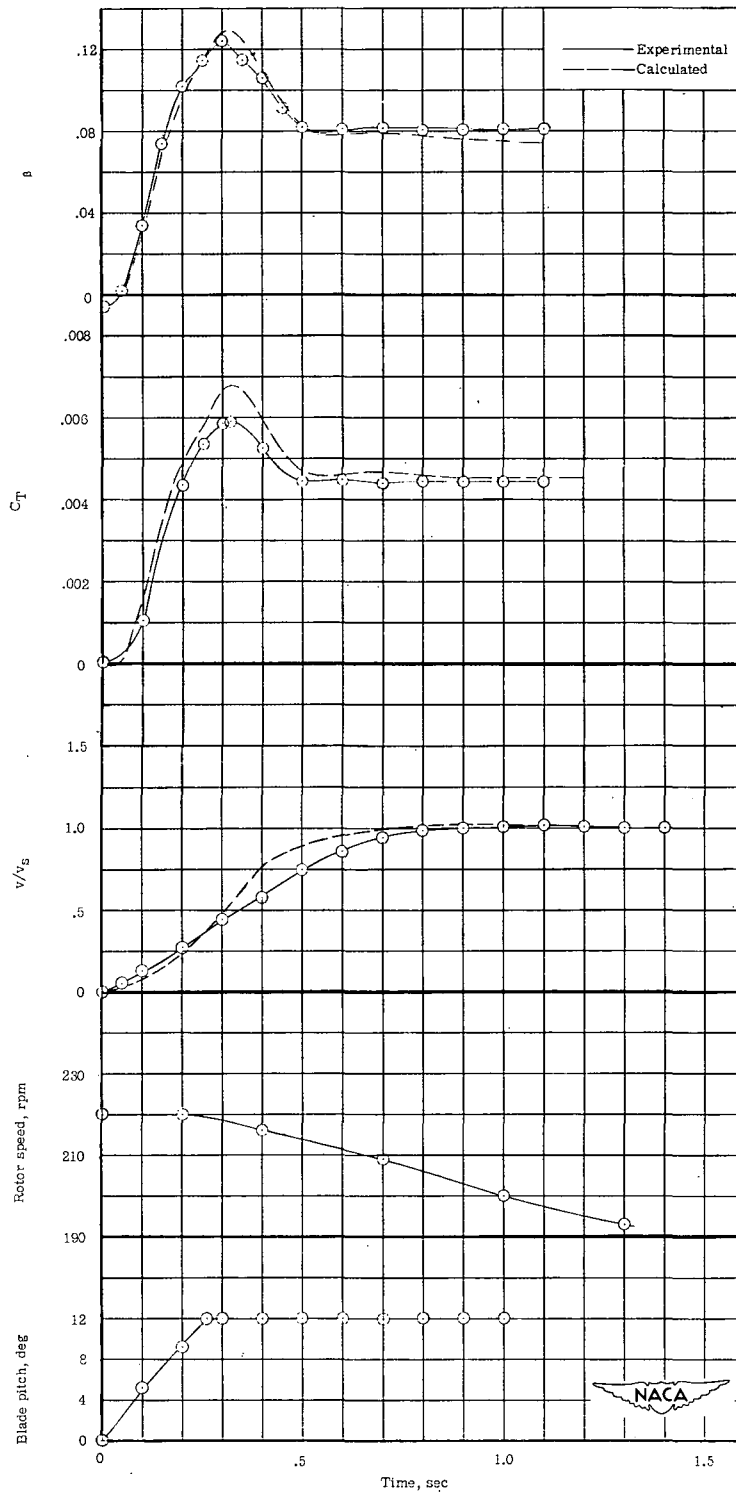
(b) Rate of pitch increase of about 48° per second.

Figure 3.- Continued.
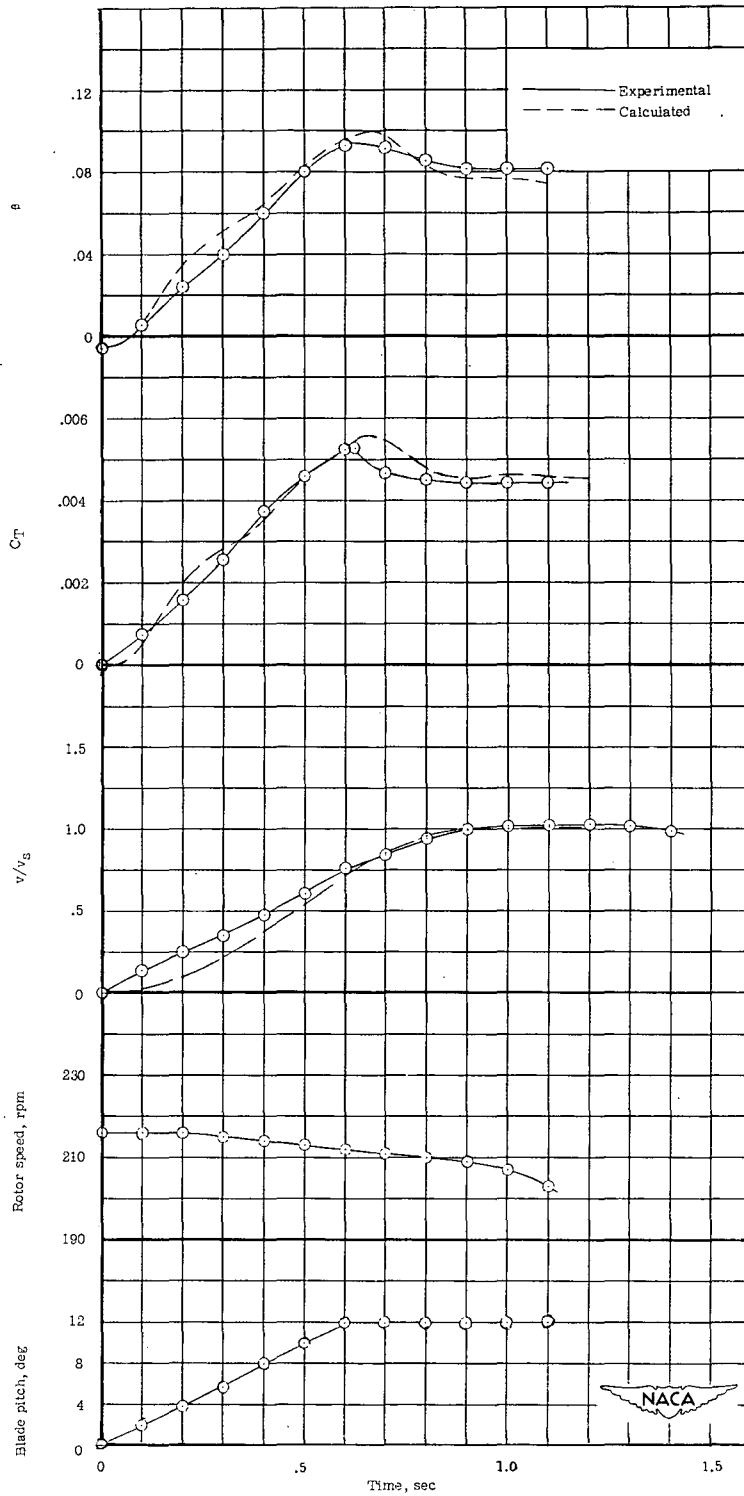
(c) Rate of pitch increase of about 20° per second.

Figure 3.- Continued.
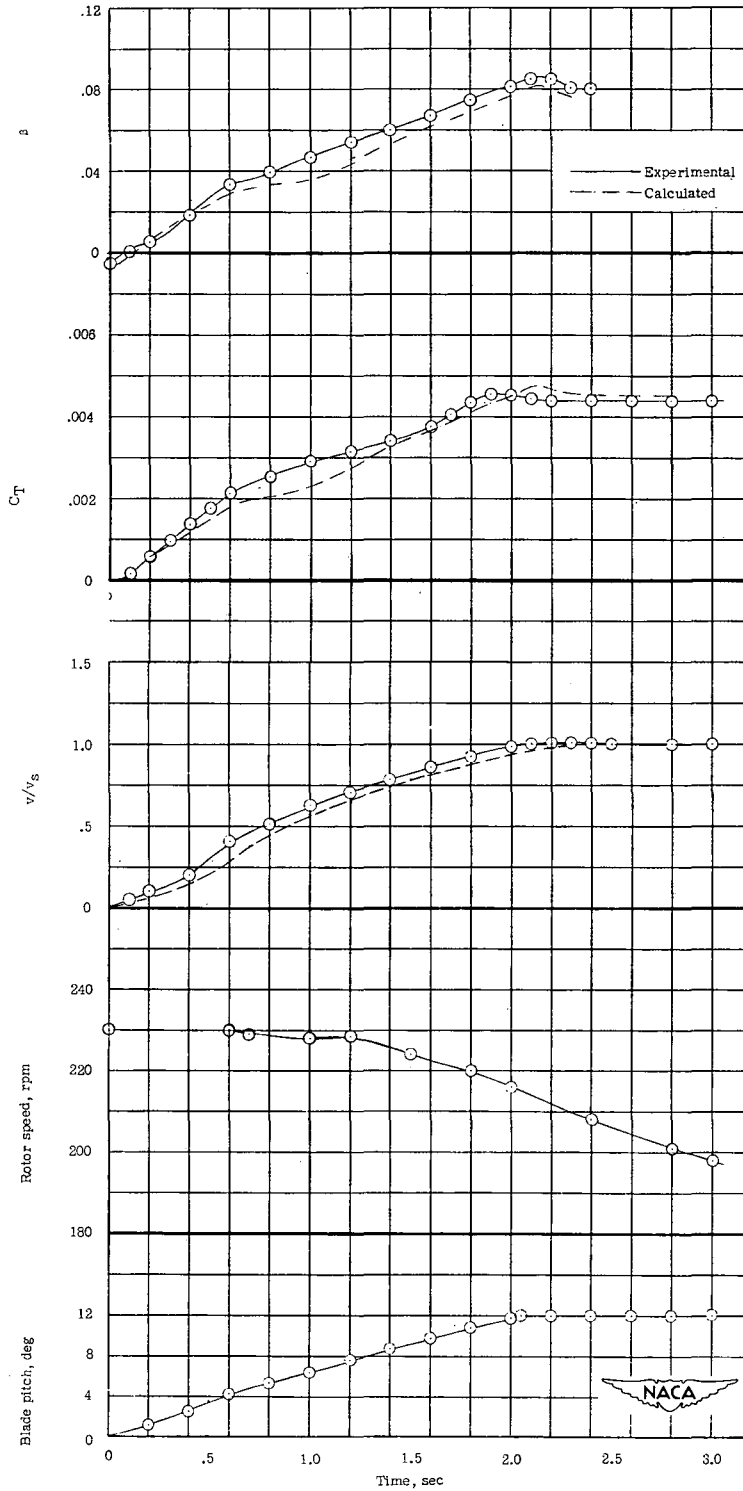
(d) Rate of pitch increase of about 6° per second.

Figure 3.- Concluded.
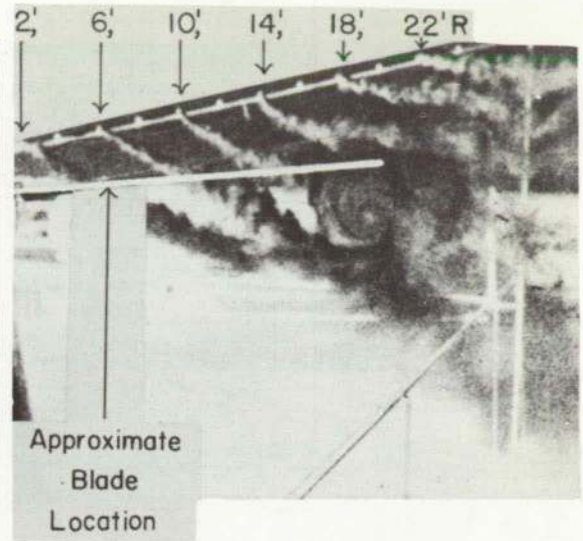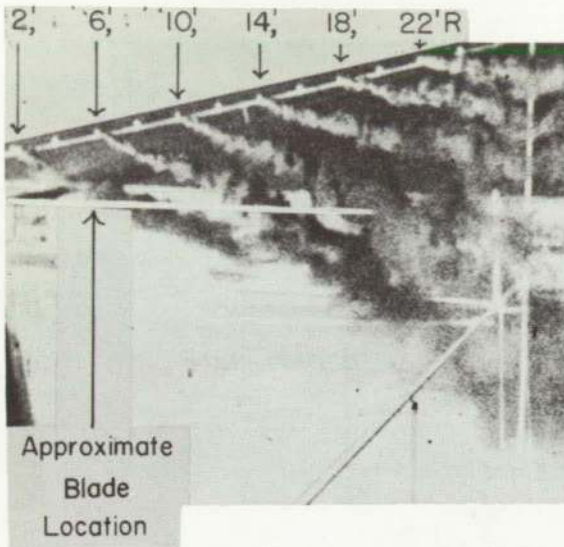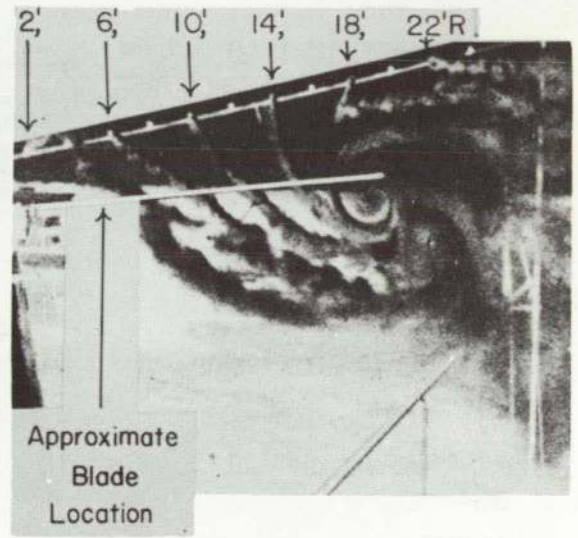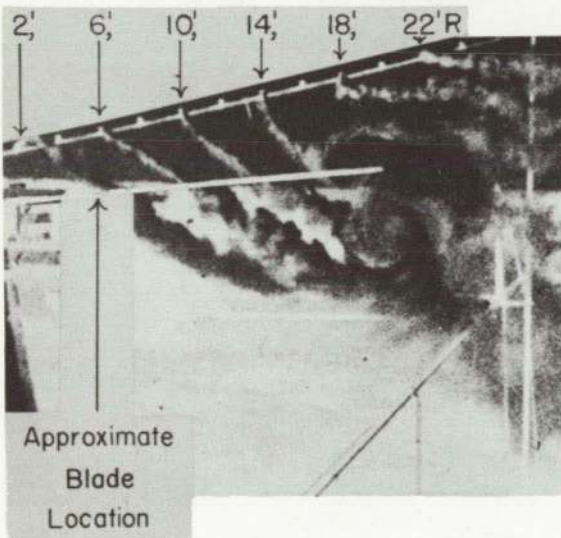
Figure 4.- Buildup of induced velocity following a very rapid pitch
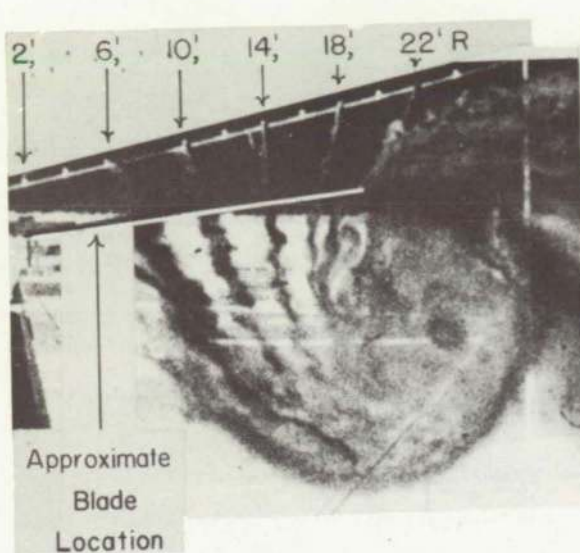change as visualized by smoke streamers.
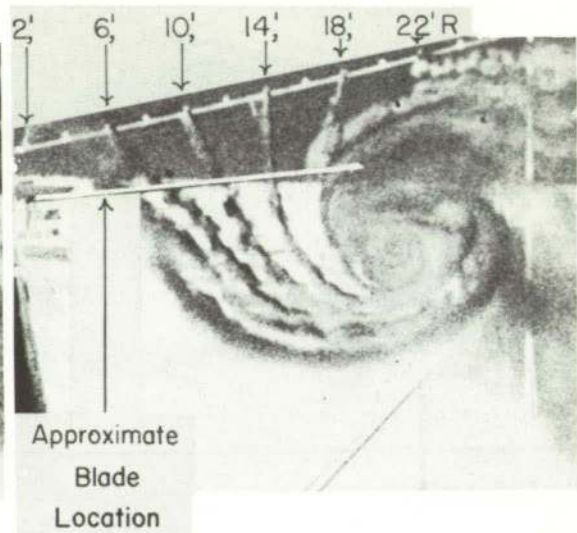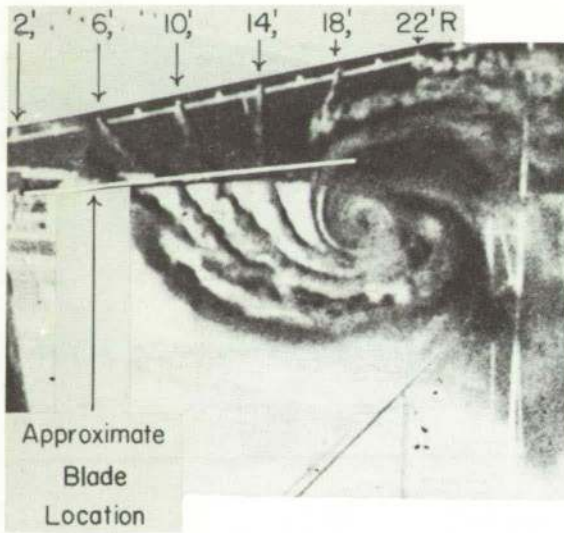
t = 0.36 sec

t = 0.45 sec
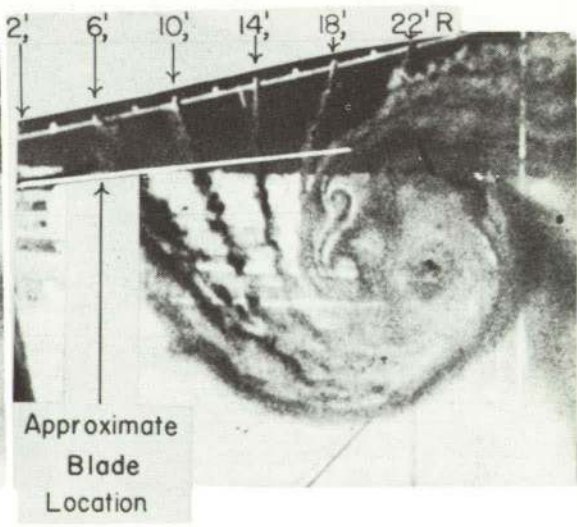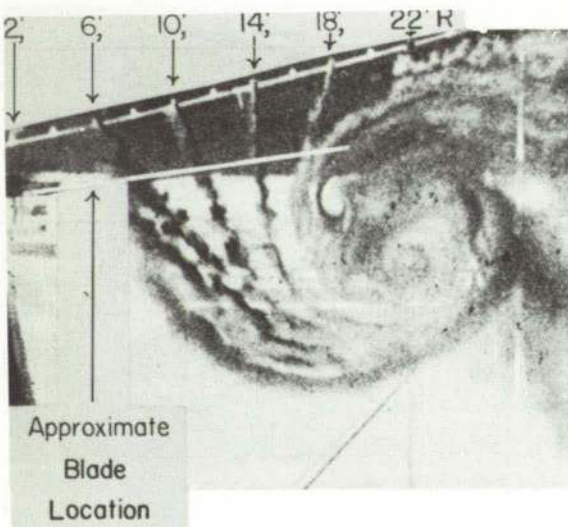


t = 0.55 sec

t = 0.64 sec          L-81189
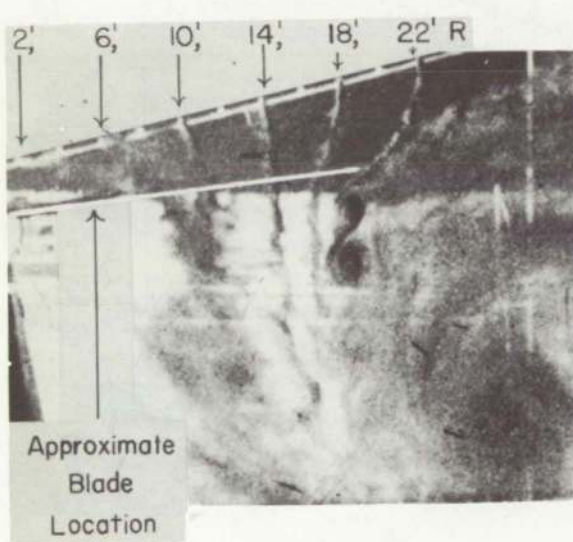
Figure 4.- Continued.
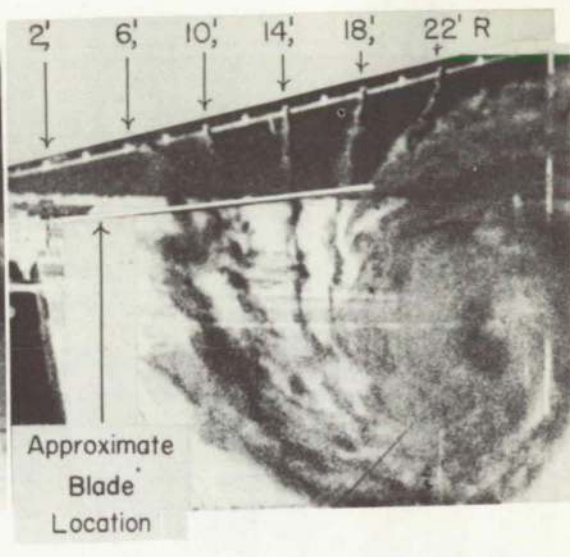
t = 0.74 sec

t = 0.91 sec
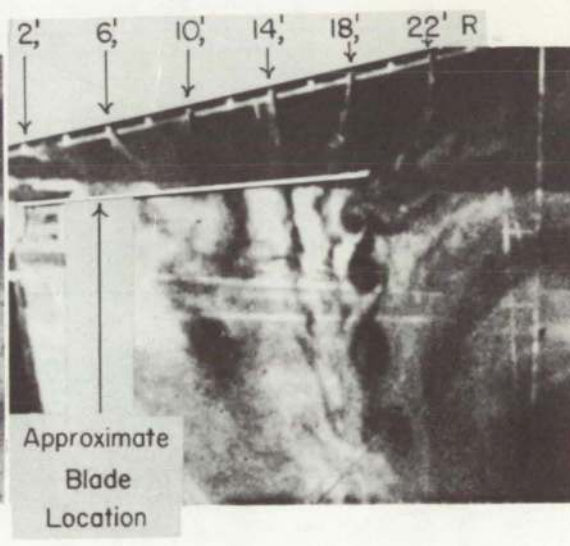
t = 1.09 sec

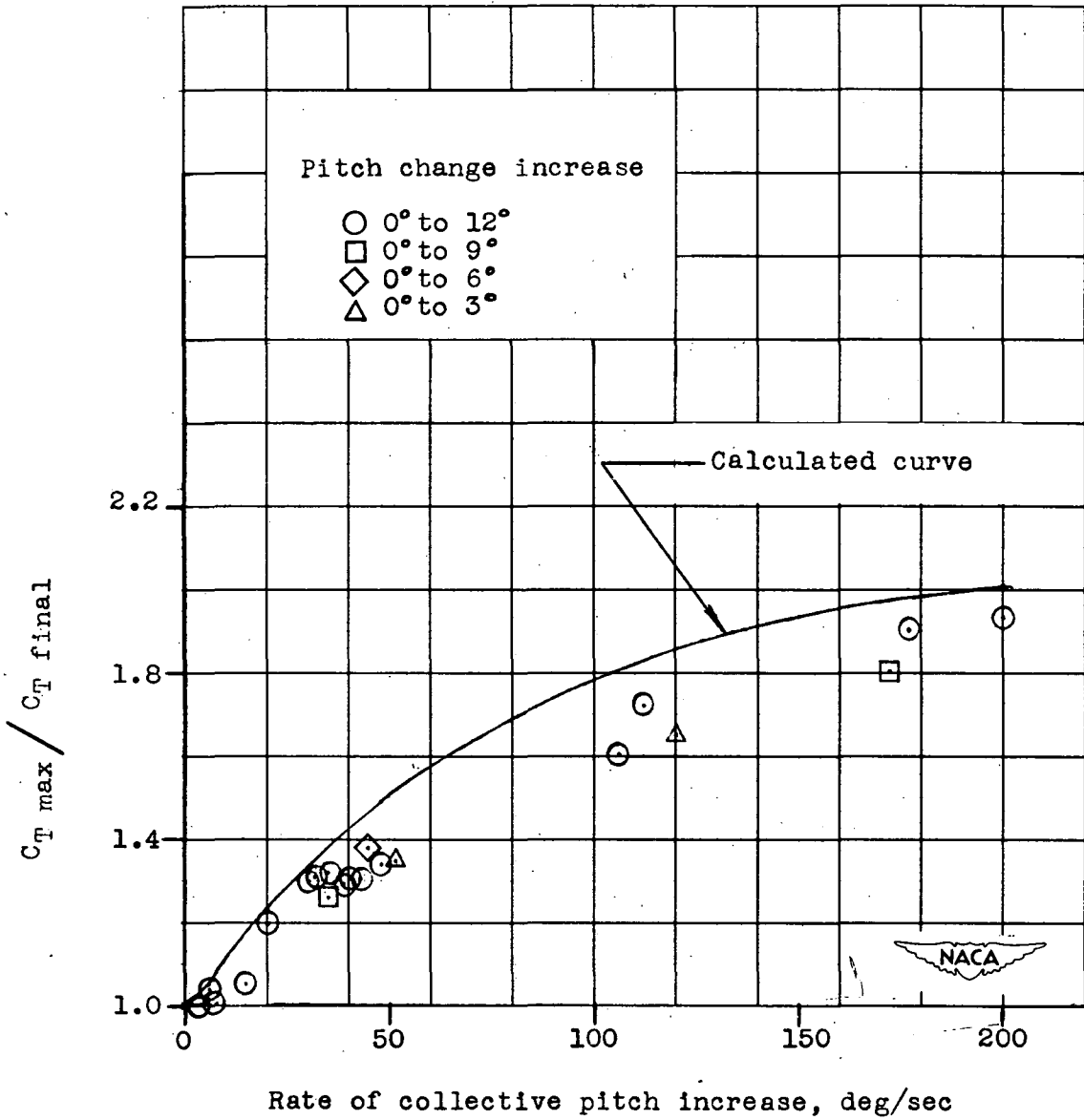t = 1.28 sec

L-81190

Figure 4.- Concluded.

Figure 5.- Comparison of experimental and calculated ratios of $C_{T_{max}}/C_{T_{final}}$ for various rates of collective pitch increase.